

A Novel Power Divider Integrated with One Bandpass Filter

Long Xiao*, Hao Peng, and Tao Yang

Abstract—A novel compact wideband inphase multilayer power divider based on slotline-to-microstrip coupling structure is presented in this paper. To improve the isolation between output ports, this power divider breaks the conventional half-wavelength slotline configuration and introduces a lumped resistor. A wideband bandpass filter integrated with the power divider is designed to allow the power divider to reject the undesired signals located in adjacent frequency channels. This filter consists of two E-shape units. In order to improve its performance at low frequency band, a lumped capacitor is bridged between the two E-shape units. As an example, a wideband power divider combining with a bandpass filter is designed and fabricated. The experimental results show that the proposed power divider has a low insertion loss, high isolation, good return losses at all ports, good amplitude and phase balance, as well as flat group delay over the wide frequency band from 3.5 GHz to 10 GHz. In addition, the width of upper stopband reaches up to 3.8 GHz (12.9 GHz–16.7 GHz) corresponding to attenuation more than 20 dB.

1. INTRODUCTION

Power divider is one of the most significant passive components in microwave and millimeter waves (MMW) systems, such as balance mixers, modulated and demodulated systems, antenna arrays, etc. As all know, Wilkinson power divider is the most classical power divider, whose relative bandwidth, usually, is less than 20%. With the study on slotline coupling structure [1–5], lots of wideband and ultra-wideband(UWB) power dividers based on slotline coupling structure have been proposed [6–11]. In [6], an UWB power divider formed by a T-junction microstrip-to-slotline coupling structure was proposed. This power divider employed traditional quarter-wavelength slotline configuration, and its output ports were combined without any compensatory circuits. Its return loss at input port was about 10 dB over the UWB frequency band 3.1 GHz–10.6 GHz. In [7], another UWB multilayer power divider with microstrip-to-slotline transition was presented. The output ports were placed in different layers and ended with circular open-circuited stubs so that the proposed power divider could obtain a flat passband and a good return loss at input port. Due to the introduction of compensatory stubs, the return loss at input port was about 12 dB, which is better than the one proposed in [6] approximately 2 dB for the same frequency band. For the power divider proposed in [10], the circular compensatory stubs were replaced by quarter-wavelength microstrip stubs. In addition, another quarter-wavelength impedance transforming microstrip line was introduced to match the input and output impedance. The return loss at input port was about 15 dB, which was better than the ones proposed in [6, 7]. In order to reject the unwanted signals while dividing signal, numerous power dividers with filtering response have been designed [12–18].

The power dividers designed in [6–11] all employed conventional half-wavelength slotline configuration, which makes the introduction of isolation resistors difficult. Because of the inherent property, a three-port network cannot obtain good impedance matching at all ports simultaneously.

Received 26 May 2014, Accepted 29 July 2014, Scheduled 31 July 2014

* Corresponding author: Long Xiao (XL740512@126.com).

The authors are with the School of Electronic Engineering, University of Electronic Science and Technology of China, UESTC, Chengdu, Sichuan 611731, China.

Therefore, the performance on return losses at output ports of these power dividers were not as good as the return losses at input ports.

In this paper, a novel wideband power divider integrated with bandpass filter is designed and fabricated. This power divider abandons traditional half-wavelength slotline structure and introduces a lumped resistor and capacitor, which makes the designed power divider show good performance on impedance matching at all ports, isolation and filtering response over a wide frequency range.

2. DESIGN OF CIRCUITS

2.1. Design of Bandpass Filter

Prior to the design of power divider, it is greatly crucial to introduce the design of bandpass filter. This bandpass filter consists of two basic units, namely E-shape units. Figure 1 shows the configuration of the E-shape unit and its equivalent circuit. This E-shape unit is formed by one short-circuited microstrip stub and two open-circuited microstrip stubs. In the E-shape unit, the two open-circuited side stubs (assuming that the middle grounded stub is removed) form a hairpin resonator. And the grounded middle stub is considered as an inductance loading the hairpin resonator at its middle like Figure 1(b) [19]. The parameters in the equivalent circuit can be obtained from following equations.

$$L_2 = \frac{Z_0 l_2 \sqrt{\varepsilon_r}}{c} \quad (1)$$

$$C_1 = \frac{(l_1 + w_b) \sqrt{\varepsilon_r}}{Z_0 c} \quad (2)$$

where ε_r , Z_0 , and c represent the dielectric constant, characteristic impedance, and the velocity of light, respectively [20]. The parameter L_1 is determined by the resonance condition of the hairpin resonator [21],

$$l_1 + w_b + s \approx \lambda_g/4 \quad (3)$$

where λ_g is the wavelength of the hairpin resonator. From the equivalent circuit, the resonant frequencies of the E-shape unit are

$$f_1 = \frac{1}{2\pi \sqrt{(2L_2 + L_1)C_1}} \quad (4)$$

$$f_2 = \frac{1}{2\pi \sqrt{L_1 C_1}} \quad (5)$$

Equations (4) and (5) for the passband edge and Equations (1)–(3) can be utilized to design a specified wideband filter.

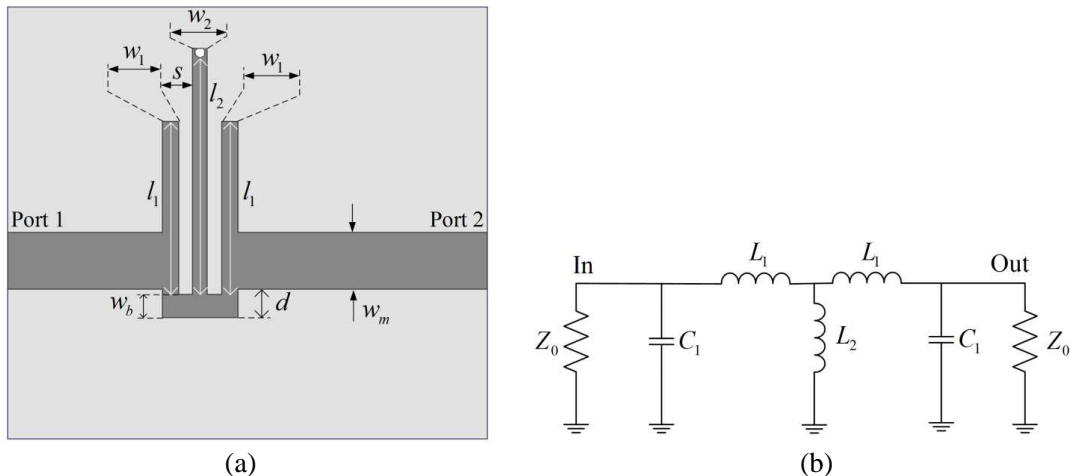


Figure 1. (a) Configuration of the E-shape unit. (b) Equivalent circuit of the E-shape unit.

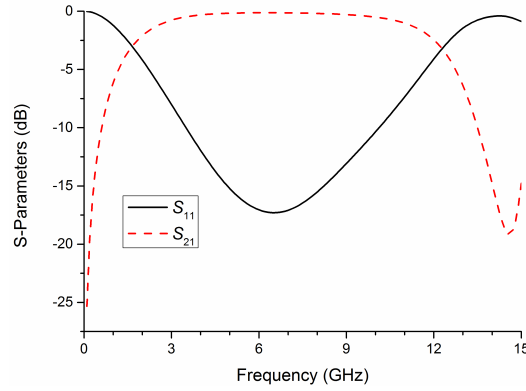


Figure 2. Simulated results of the E-shape unit.

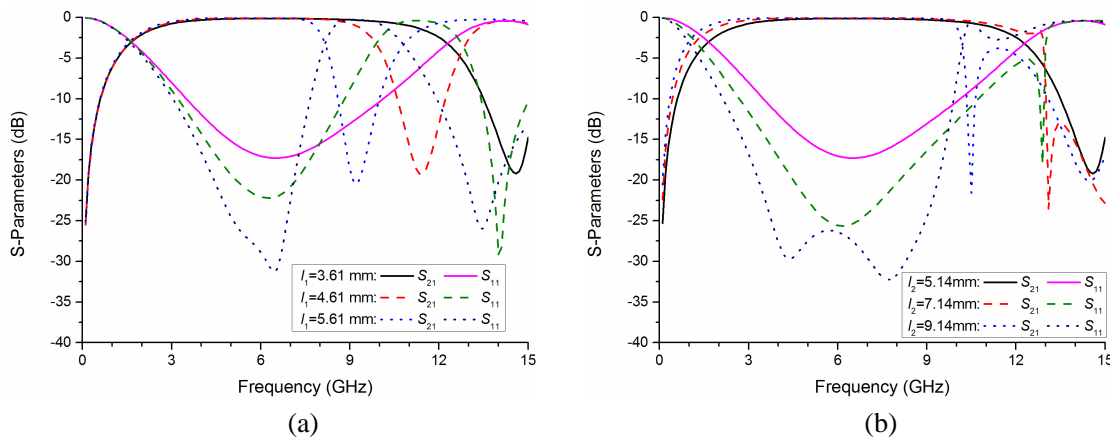


Figure 3. Frequency response to different parameters. (a) Frequency response to different lengths of l_1 . (b) Frequency response to different lengths of l_2 .

According to the design principles mentioned above, a filter with bandpass property can be obtained. This is demonstrated using an E-shape unit with (unit: mm): $w_1 = 0.34$, $w_2 = 0.3$, $w_b = 0.48$, $w_m = 1.17$, $l_1 = 3.61$, $l_2 = 5.14$, $s = 0.3$, $d = 0.6$. In this example, the E-shape unit is fabricated on Rogers 4003C with dielectric constant of 3.38, dielectric loss tangent of 0.0027, thickness of 0.508 mm.

Basing on the values of the parameters and the above equations, the element values could be worked out as: $L_2 = 3.15$ nH, $C_1 = 0.26$ pF, $L_1 = 0.97$ nH. Thus the resonance frequencies are $f_1 = 3.66$ GHz, $f_2 = 10.0$ GHz.

The simulated data over the range from 0.1 GHz to 15 GHz is exhibited in Figure 2. It is noticeable that the resonance frequencies f_1 and f_2 are close to the passband edge frequencies 3.5 GHz and 10.1 GHz corresponding to the insertion loss less than 0.4 dB, which reveals that the design principle is reasonable.

The resonance point can be controlled by adjusting the length of short-circuited and open-circuited stubs. Figures 3(a) and (b) show the simulated results about the frequency response to different lengths of l_1 and l_2 . It is easy to find that the change of l_1 and l_2 will influence the frequency response. The resonance point will move towards lower frequency band with l_1 or l_2 decreasing. However, the change of l_2 will not only influence the resonance point, but also influence the transmission coefficient and the width of upper stopband.

In order to obtain a wider stopband and a greater attenuation in stopband, a new wide bandpass filter consisting of two E-shape units is designed. The two E-shape units are placed closely so that the electromagnetic wave can be coupled from one E-shape unit to the other. Figure 4 exhibits the configuration of wide bandpass filter, and Figure 5 shows its simulation results. The distance between the two E-shape units g is selected to be 0.05 mm. Analyzing Figure 5, we can find that the width of

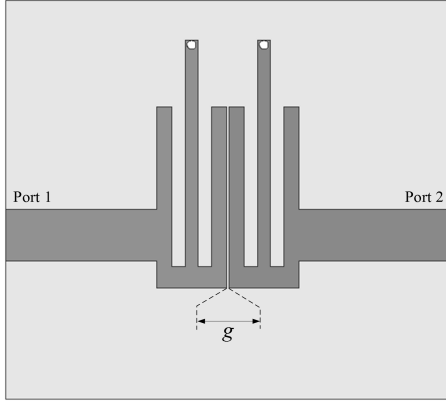


Figure 4. Configuration of the wide bandpass filter.

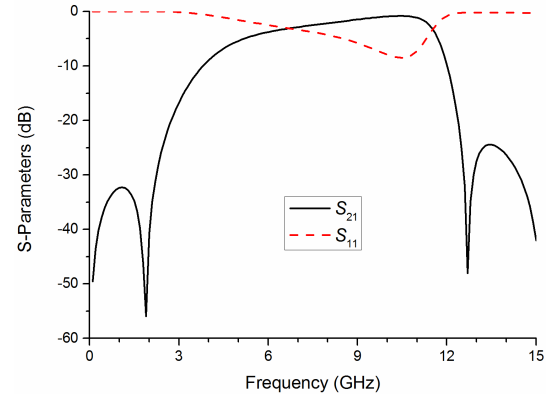


Figure 5. Simulation results of the wide bandpass filter.

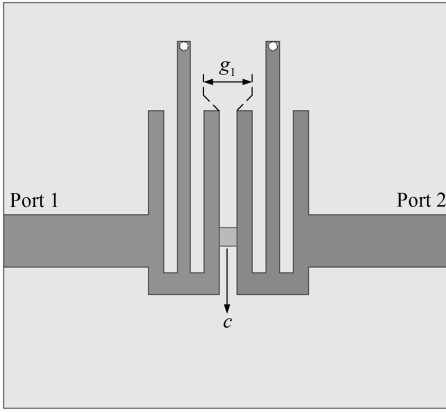


Figure 6. Configuration of wideband bandpass filter with lumped capacitor.

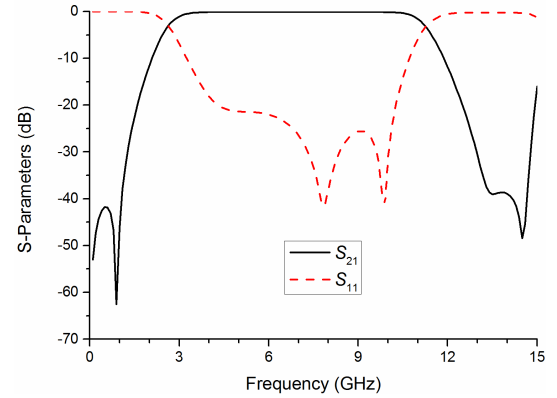


Figure 7. The simulated insertion loss of filter with lumped capacitor.

upper stopband has been broadened, and a new resonance point has been generated at low frequency band. Nevertheless, because the coupling effect is not satisfactory at low passband, the insertion loss in low passband is greater than the one in high passband as shown in Figure 5. What's worse, its standing wave is greatly terrible. As all know, the shorter the distance is, the stronger the coupling can be obtained. However, it is difficult to manufacture a narrow gap for current processing technic.

To obtain a good passband with low insertion loss and a realizable circuit for current processing technic, a lumped capacitor is introduced and soldered across the two E-shape units as is exhibited in Figure 6. The gap between the two E-shape units is broadened which is favorable for manufacture because of the introduction of the lumped capacitor. Moreover, the insertion loss at low passband, shown in Figure 7, is also improved in comparison with the one exhibited in Figure 5. In the simulation about the filter with lumped capacitor, the gap g_1 is chosen to be 0.4 mm which is eight times wider than the one without lumped capacitor, and the value of lumped capacitor c is selected as 0.5 pF. The other dimensions are the same as the ones in Figure 1.

2.2. Design of Power Divider Integrated with Bandpass Filter

The power divider integrated with bandpass filter is exhibited in Figure 8. It consists of three layers. The input port and integrated bandpass filter are placed in bottom layer. The output ports are placed in the top layer, while the slotline is etched in the ground plane. The slotline employs a shorter dimension to replace the conventional half-wavelength dimension so that the lumped resistor can be placed properly

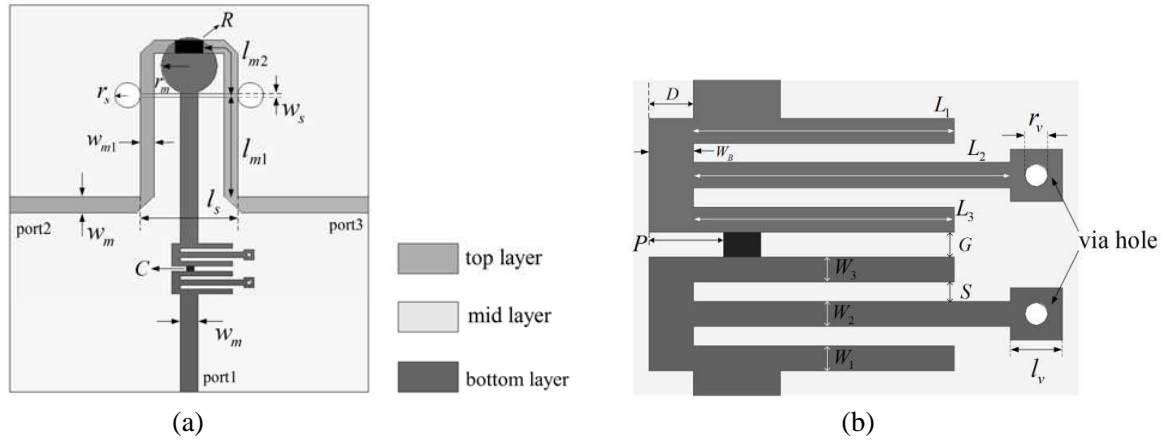


Figure 8. Configuration of the proposed novel power divider. (a) Dimensions of the power divider. (b) Dimensions of the integrated bandpass filter.

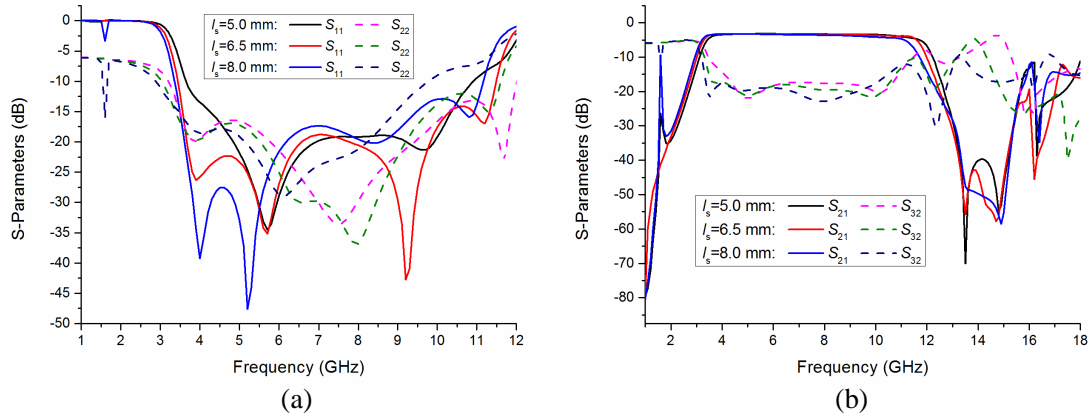


Figure 9. The influence of l_s on frequency response. (a) Influence on return losses at input and output ports. (b) Influence on insertion loss and isolation.

between output branches. One circular microstrip stub and two circular slotline stubs are designed to improve the performance of the presented power divider. In order to obtain good impedance matching between microstrip line and slotline, their characteristic impedances should satisfy (6).

$$Z_m = n^2 \times Z_s \quad (6)$$

where Z_m , Z_s , and n are the characteristic impedance of microstrip line, characteristic impedance of slotline, and coupling coefficient between microstrip line and slotline.

r_m and r_s stand for the radius of the capacitive circular microstrip stub and inductive slotline circular stub, respectively. They are usually selected to be approximately $\lambda_m/12$ and $\lambda_s/12$. λ_m and λ_s are the guided wavelength of microstrip line and slotline at center frequency, respectively. l_{m1} and l_{m2} are usually chosen as a quarter wavelength. In most previous designs, the length of slotline, l_s , was selected to be half wavelength. However, in this design it has a shorter length so that the resistor can be soldered on the output stubs. As to the width w_{m1} , it associates with the output impedance, because it is utilized to convert the output impedance to 50Ω .

To understand the influence of parameters on the power divider in an even better fashion, some simulation studies are done as shown in Figures 9–13. The impact of the length of slotline l_s on frequency response is researched in Figure 9. The impact from the variation of l_s on the standing waves at input and output ports is little, which can be obtained by analyzing the return losses (S_{11} and S_{22}) shown

in Figure 9. Studying Figure 9(b), we can find that the impact of l_s on isolation between output ports (S_{32}) and the passband (S_{21}) is negligible, but the change of l_s will influence the stopband. For instance, one transmission pole will be generated at the frequency point 1.6 GHz when the length of slotline equal 8.0 mm.

In Figure 10, the impact of r_s on the response frequency has been researched. Compared with the impact from l_s , the impact from r_s should not be negligible. The variation of r_s not only makes the impedances at input and output port mismatching, but also affects the isolation. The influence on insertion loss is slight compared with the impact on the parameters.

In Figure 11, the influence of r_m on return losses at input port and output ports as well as the insertion loss is similar to the parameter r_s . Nevertheless, the impact from r_m on isolation is less than the one from r_s .

In Figure 12, the influence of the width of output branch w_{m1} has been studied. As mentioned above, the output branch is one impedance-transformation microstrip line. Thus the variation of w_{m1} will make all ports mismatching. In other words, the performance of return losses at all ports will be worsened no matter increasing the size or decreasing the size of w_{m1} .

Another parameter l_{m2} , the length of microstrip stub, has been studied, too. Compared with the parameter w_{m1} , its influence on return losses at all ports and insertion loss is similar. The difference

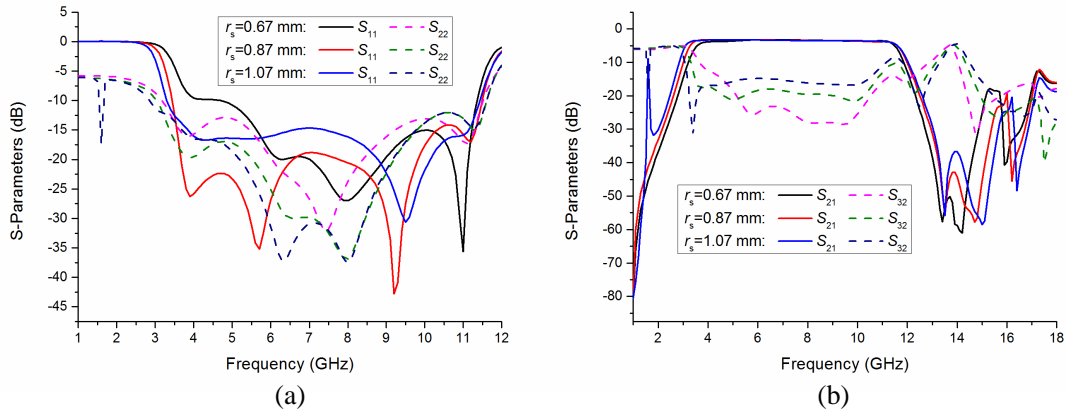


Figure 10. The influence of r_s on frequency response. (a) Influence on return losses at input and output ports. (b) Influence on insertion loss and isolation.

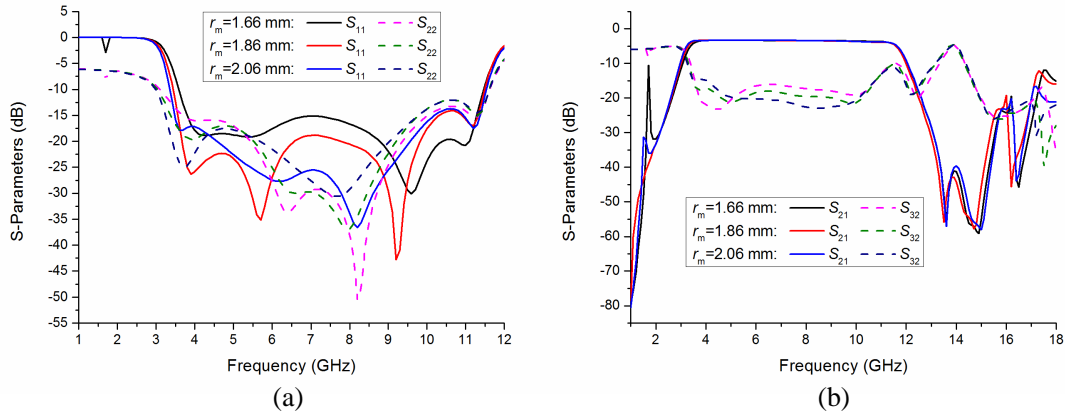


Figure 11. The influence of r_m on frequency response. (a) Influence on return losses at input and output ports. (b) Influence on insertion loss and isolation.

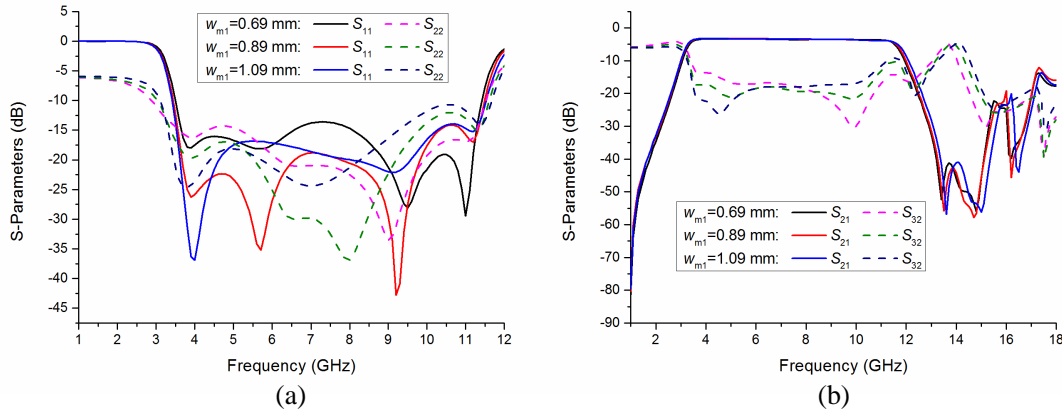


Figure 12. The influence of w_{m1} on frequency response. (a) Influence on return losses at input and output ports. (b) Influence on insertion loss and isolation.

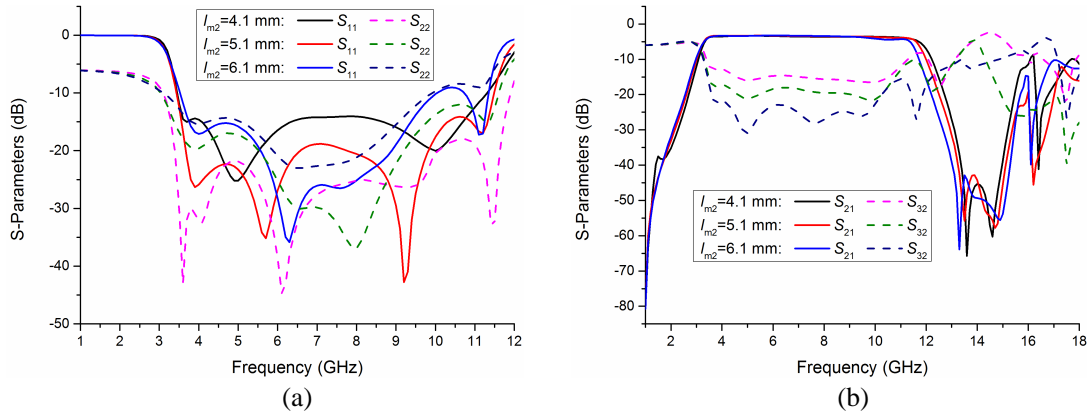


Figure 13. The influence of l_{m2} on frequency response. (a) Influence on return losses at input and output ports. (b) Influence on insertion loss and isolation.

between them is that the impact on isolation between output ports is greater than that from w_{m1} as shown in Figure 13.

3. SIMULATED AND MEASURED RESULTS

The proposed compact wideband power divider with bandpass response and high isolation is fabricated on Rogers 4003C with dielectric constant 3.38, thickness 0.508 mm, and loss tangent 0.0023. Figure 14 exhibits a photograph the novel power divider. The dimension of the compact power divider is 24 mm × 26 mm. The practical dimensions of the relative parameters are listed as (unit: mm): $l_{m1} = 6.81$, $l_{m2} = 5.1$, $r_m = 1.86$, $r_s = 0.87$, $w_s = 0.23$, $w_{m1} = 0.89$, $w_m = 1.16$, $l_s = 6.5$, $D = W_B = 0.6$, $P = 1$, $L_1 = L_3 = 3.5$, $L_2 = 4.75$, $W_1 = W_3 = 0.33$, $W_2 = 0.34$, $G = 0.34$, $S = 0.26$, $r_v = 0.15$, $l_v = 0.7$. In addition, the lumped resistor and capacitor are selected $R = 100 \Omega$ and $C = 0.5$ pF.

In order to comprehend the performance of the filter, the simulated results of the power divider without filter are exhibited in Figure 15. Comparing it with the results with filter shown in Figure 16, we can find that the return losses at all ports and isolation are analogous, while the attenuation in the upper stopband has been worsened.

Figure 16 exhibits the simulated and measured data of the proposed novel power divider integrated with a wideband bandpass filter. The return losses at input port and output port as well as the isolation are exhibited in Figure 16(a) for the range from 1 GHz to 12 GHz. The simulated return loss at input

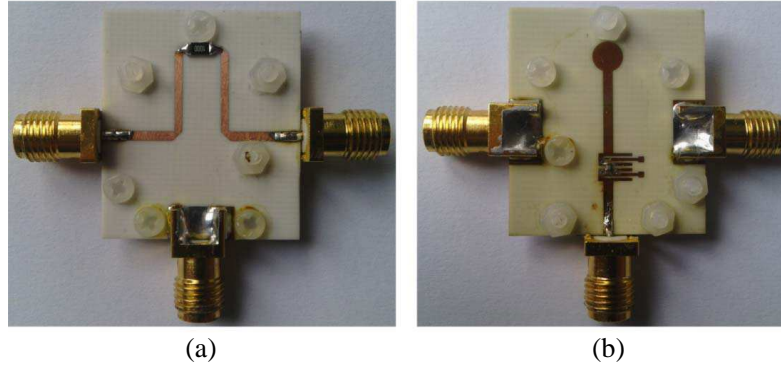


Figure 14. Photograph of the proposed power divider. (a) Top view. (b) Bottom view.

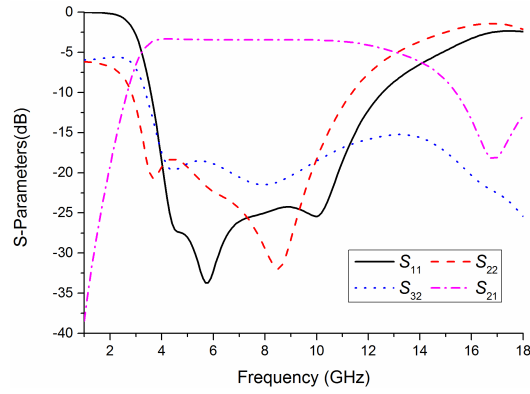


Figure 15. Simulated results of the proposed power divider without filter.

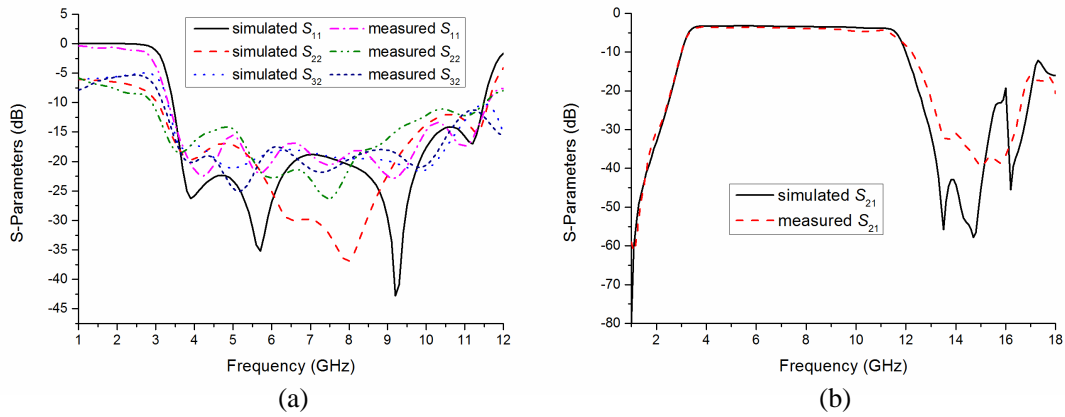


Figure 16. Simulated and measured results of the presented power divider. (a) Return losses and isolation. (b) Insertion loss.

port (S_{11}) is approximately 20 dB, while the measured one is about 17.5 dB over the band 3.5 GHz–10.0 GHz. The simulated return loss at output port (S_{22}) is greater than 15 dB over the frequency range 3.3 GHz–10.0 GHz, while the measured one is superior to 13 dB for the same range. The simulated and measured isolations (S_{32}) are more than 18 dB for the band 3.5 GHz–10.0 GHz. Observing the simulated and measured data (for instance, S_{11} and S_{22}), we can find that the simulated and measured data show a good agreement and that the simulated data are mainly superior to the measured ones. The difference

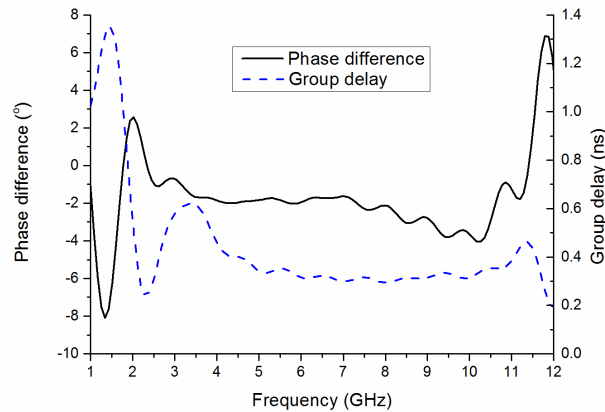


Figure 17. Group delay and phase difference of the presented power divider.

Table 1. Comparison between proposed slotline power divider and other slotline power dividers.

References	[6]	[9]	[17]	[18]	This work
Frequency (GHz)	3.1–10.6	3.1–10.6	3.5–10.1	3.1–10.0	3.5–10.0
Return loss S_{11}/S_{22} (dB)	10/8	14/10	10/10	10/10	17.5/13
Insertion loss (dB)	0.5	0.8	2	2	1.4
Isolation (dB)	8	9	10	10	18

between them mainly results from machining error and soldering error.

The experimental data of insertion loss (S_{21}) have been obtained over the band 1 GHz–18 GHz in Figure 16(b). It is obvious that the measured and simulated insertion losses are about 1 dB for the passband 3.5 GHz–11.5 GHz. In addition, the width of upper stopband reaches up to 3.8 GHz (from 12.9 GHz to 16.7 GHz) corresponding to attenuation more than 20 dB for the measured result.

Figure 17 shows the measured phase difference and group delay over the range 1.0 GHz–12.0 GHz. For the band 3.5 GHz–10.0 GHz, the phase difference is within the range -4° – -1° , and the group delay is greatly flat with maximum fluctuate of 0.2 ns.

Table 1 lists the presented slotline power divider and the previous slotline power dividers. By introducing one lumped resistor, the presented power divider's return losses and isolation have been improved greatly. The integration of wideband filter makes the presented divider has a wide upper stopband, which makes it outdistance the previous ones designed in [6–11].

4. CONCLUSION

A novel compact slotline power divider integrated with a wideband filter is designed. The combination of distribution-parameter circuits and lumped components has made the performance on isolation and filtering response improved. The impact of the parameters on the frequency response has been analyzed and studied. The experimental results indicate that the presented slotline power divider has good performance on insertion loss, return loss, phase balance as well as group delay over the range 3.5 GHz–10 GHz. In addition, the width of upper stopband reaches up to 3.8 GHz corresponding to attenuation greater than 20 dB.

ACKNOWLEDGMENT

This work was sponsored by the National Natural Science Foundation of China (Grant No. 61006026).

REFERENCES

1. Cohn, S. B., "Slot line on a dielectric substrate," *IEEE Trans. Microw. Theory Tech.*, Vol. 17, No. 10, 768–778, 1969.
2. Knorr, J. B., "Slot-line transitions," *IEEE Trans. Microw. Theory Tech.*, Vol. 22, No. 5, 548–554, 1974.
3. Schuppert, B., "Microstrip/slotline transitions: Modeling and experimental investigation," *IEEE Trans. Microw. Theory Tech.*, Vol. 36, No. 8, 1272–1282, 1988.
4. Zinieris, M. M., R. Sloan, and L. E. Davis, "A broadband microstrip-to-slot-line transition," *Microw. Opt. Tech. Lett.*, Vol. 18, No. 5, 339–342, 1988.
5. Wang, N. B., Y. C. Jiao, L. Zhang, Y. Song, and F. S. Zhang, "A simple low-loss broadband 1–14 GHz microstrip-to-slotline transition," *Microw. Opt. Tech. Lett.*, Vol. 51, No. 9, 2236–2239, 2009.
6. Bialkowski, M. E. and A. M. Abbosh, "Design of a compact UWB out-of-phase power divider," *IEEE Microw. Wireless Compon. Lett.*, Vol. 17, No. 4, 289–291, 2007.
7. Bialkowski, M. E., A. M. Abbosh, and N. Seman, "Compact microwave six-port vector voltmeters for ultra-wideband applications," *IEEE Trans. Microw. Theory Tech.*, Vol. 55, No. 10, 2216–2223, 2007.
8. Abbosh, A. M., "Multilayer inphase power divider for UWB applications," *Microw. Opt. Tech. Lett.*, Vol. 50, No. 5, 1402–1405, 2008.
9. Li, Q., X. W. Shi, F. Wei, and J. G. Gong, "A novel planar 180° out-of-phase power divider for UWB application," *Journal of Electromagnetic Waves and Applications*, Vol. 25, No. 1, 161–167, 2011.
10. Song, K. J. and Q. Xue, "Ultra-wideband out-of-phase power divider using multilayer microstrip-slotline coupling structure," *Microw. Opt. Tech. Lett.*, Vol. 52, No. 7, 1591–1594, 2010.
11. Peng, H., Z. Q. Yang, Y. Liu, T. Yang, and K. Tan, "An improved UWB non-coplanar power divider," *Progress In Electromagnetics Research*, Vol. 138, 31–39, 2013.
12. Cheong, P., K. I. Lai, and K. W. Tam, "Compact Wilkinson power divider with simultaneous bandpass response and harmonic suppression," *2010 IEEE MTT-S International Microwave Symposium Digest*, 1588–1591, 2010.
13. Gao, L. and X. Y. Zhang, "Novel 2 : 1 Wilkinson power divider integrated with bandpass filter," *Microw. Opt. Tech. Lett.*, Vol. 55, No. 3, 646–648, 2013.
14. Chau, W. M., K. W. Hsu, and W. H. Tu, "Wide-stopband Wilkinson power divider with bandpass response," *Electron. Lett.*, Vol. 50, No. 1, 39–40, 2014.
15. Singh, P. K., S. Basu, and Y. H. Wang, "Coupled line power divider with compact size and bandpass response," *Electron. Lett.*, Vol. 45, No. 17, 892–894, 2009.
16. Song, K. J., X. Ren, F. L. Chen, and Y. Fan, "Ultra wideband notch-band power divider with bandpass response using defect microstrip structure," *Microw. Opt. Tech. Lett.*, Vol. 56, No. 3, 711–715, 2014.
17. Wong, S. W. and L. Zhu, "Ultra-wideband power divider with good in-band splitting and isolation performances," *IEEE Microw. Wireless Compon. Lett.*, Vol. 18, No. 8, 518–520, 2008.
18. Song, K. J. and Q. Xue, "Novel ultra-wideband (UWB) multilayer slotline power divider with bandpass response," *IEEE Microw. Wireless Compon. Lett.*, Vol. 20, No. 1, 13–15, 2010.
19. Hammed, R. T. and D. Mirshekar-Syahkal, "High-order UWB bandpass filter using cascaded E-shape microstrip structure," *2011 IEEE MTT-S International Microwave Symposium Digest*, 1–4, 2011.
20. Hong, J. S. and M. J. Lancaster, *Microstrip Filter for RF/Microwave Applications*, Wiley, New York, 2001.
21. Hammed, R. T. and D. Mirshekar-Syahkal, "A lumped element equivalent circuit of E-shape microstrip structure for UWB filter design," *2011 41st European Microwave Conference (EuMC)*, 651–654, 2011.